PHYSICAL REVIEW B VOLUME 26, NUMBER 8 15 OCTOBER 1982

Electronic structure of carbon intercalated atoms in graphite. A single-layer approach

C. Priester and G. Allan
Laboratoire de Physique des Solides, Institut Superieur d'Electronique du Nord, 3, rue François Baës, 59046 Lille Cedex, France*
J. Conard
Centre de Recherche sur les Solides à Organisation Cristalline Imparfaite— Centre National de la Recherche Scientifique, 45045 Orleans Cedex, France

(Received 16 November 1981)

In the tight-binding approximation we calculate the electronic structure of carbon atoms intercalated between graphite layers. These interstitial carbons induce variation of the density of states which agree quite well with the few experimental data available. The energy and the equilibrium position of the interstitial atom are also compared with the measured values. We also show that the interstitial energy rapidly decreases when one adds a small amount of boron substitutional impurities. The interstitial carbons also considerably increase the density of states at the Fermi level as in other intercalated compounds.

I. INTRODUCTION

Perfect graphite has very small density of states at the Fermi level.[1] That provides a moderately good conductivity parallel to the atomic layers. Owing to its lamellar structure, it presents many intercalation compounds. These consist of stacks of one or more hexagonal carbon atom layers alternating with monolayers of guest atoms or molecules (Li, I, K, AsF_5, HNO_3, etc.). These compounds are extensively investigated owing to their mechanical and electrical properties and their technological applications.[2–7] We have studied the electronic structure of interstitial carbons between the graphitic layers. In fact, when one makes graphite, carbon point defects frequently occur. A few years ago, x-ray diffusion experiments[8] have shown the existence of these defects and measured the position of these interstitials. We will show later that the interaction between the interstitials is very weak. This explains why we have only point defects, and not a well-defined intercalation compound such as LiC_6 or KC_8.

In the next section, we calculate the perfect graphite electronic structure in the tight-binding approximation limited to nearest neighbors. This allows us to fit the tight-binding parameters to existing band structures.[9–12] As it has been established[12] that for a first approach, the two-dimensional graphite structure model gives results in good agreement with the experimental interband transitions we will use the two-dimensional and nearest-neighbor approximation. So we have then a very simple model that allows us to study the influence of the interstitials. We also show that the interaction between atoms belonging to different layers is small and that the interstitial carbons at their equilibrium position mainly interact with only one graphite layer. For a very small concentration of interstitials, we calculate the influence of interstitial carbons upon the density of states by the Green's-function formalism.[13] Some of our results well agree with the secondary electron spectra.[14] Then we deduce the interstitial energy and its equilibrium position. These values also are close to the experimental ones. Moreover, we show that the energy greatly depends on the graphite Fermi level. For example, it rapidly decreases with a very small amount of acceptor such as boron substitutional impurities.

At larger interstitial concentrations the interaction between the nearest-neighbor intercalated carbon atoms remains small. Nevertheless, the density of states at the Fermi level is considerably larger than in pure graphite. Then the conductivity parallel to the graphite layers is certainly modified.[15] Neverthelsss, as the interaction between layers remains small, it certainly will not be equal to the expected values for other intercalated compounds like LiC_6 or KC_8.

II. GRAPHITE ELECTRONIC STRUCTURE

The tight-binding approximation seems well suited to study the graphite electronic structure. At least it gives a good description of the valence

bands of diamond or of other covalent semiconductors such as silicon or germanium. The simplicity of the calculations allows us to calculate defect properties like vacancies, surfaces, or interstitials. Let us briefly recall here the used approximations.

Using the periodicity of the crystal, the nth eigenfunction $\Psi^n_{\vec{k}}$ of the one-electron perfect-lattice Hamiltonian H is expressed as linear combination of Bloch waves $\phi^i_{\vec{k}}(\vec{r})$:

$$H\Psi^n_{\vec{k}}=E_n(\vec{k})\Psi^n_{\vec{k}}\ , \tag{1}$$

$$\Psi^n_{\vec{k}}(\vec{r})=\sum_i C_{n,i}(\vec{k})\phi^i_k(\vec{r})\ , \tag{2}$$

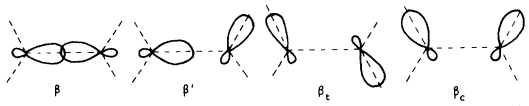

FIG. 1. Two-center integrals between hybridized sp_2 orbitals for atoms belonging to the same graphite layer.

where $\vec{k}$ is the wave vector and $E_n(\vec{k})$ the energy. The summation in the expression (2) is extended to all the Bloch waves which are defined as

$$\phi^i_{\vec{k}}(\vec{r})=\frac{1}{\sqrt{N}}\sum_j e^{i\vec{k}\cdot\vec{R}_j}\Phi_i(\vec{r}-\vec{R}_j)\ , \tag{3}$$

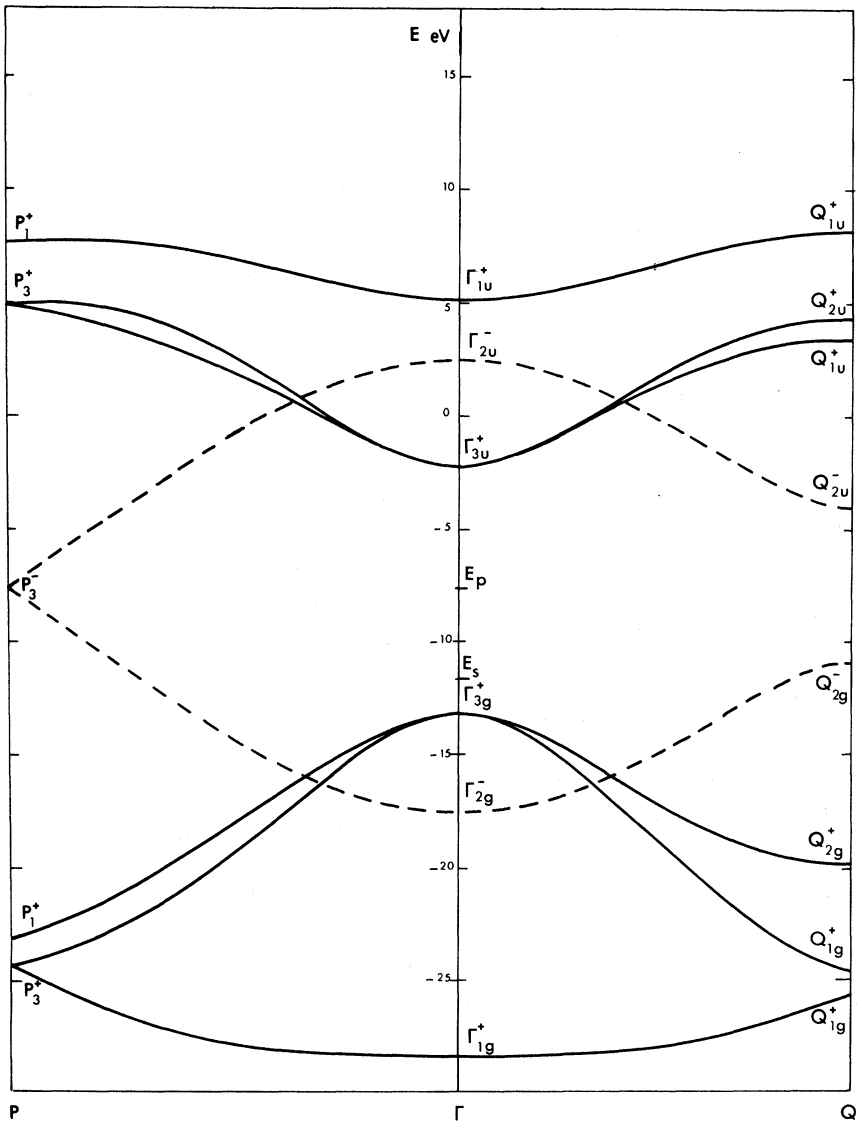

FIG. 2. Graphite energy dispersion curves (zero energy is given by the fit on Painter and Ellis results).

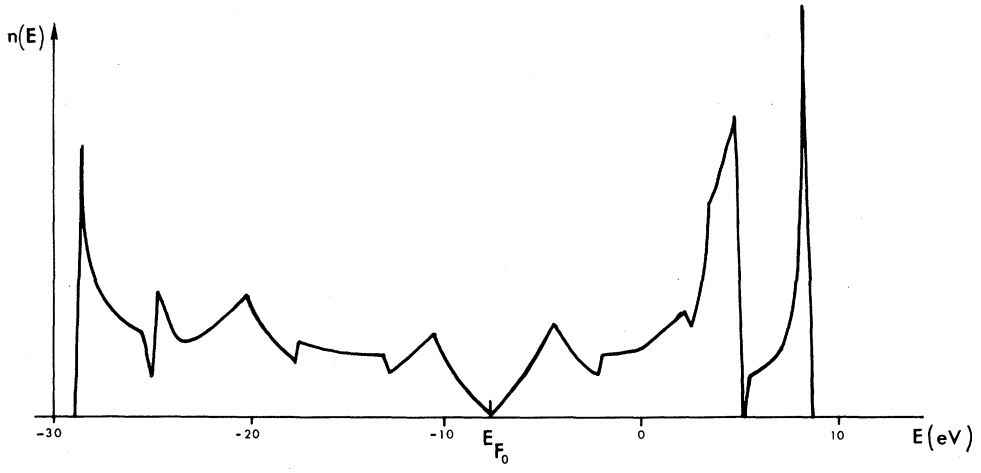

FIG. 3. Graphite density of states. (Fermi level E_{F_0} is at E_p.)

where $\Phi_i(\vec{r}-\vec{R}_j)$ is an atomic orbital centered on the lattice site R_j and N is the crystal atom number. The atomic orbitals are also assumed to be orthogonal for orbitals on different sites. We here consider four orbitals per atom (one s and three p states). If we consider only interactions between atoms in the same layer, the Hamiltonian for a given wave vector $\vec{k}$ is easily obtained as a function of the s and p atomic levels E_s and E_p and of the usual two-center integrals β_{ss}, $\beta_{\sigma\sigma}$, $\beta_{\sigma s}$, and $\beta_{\pi\pi}$. In an sp_2 hybridized basis of orbitals centered on one atom and pointing along the nearest-neighbor directions, we define four two-center integrals between hybridized orbitals β, β', β_t, and β_c (Fig. 1). The parameters, fitted on the Painter and Ellis band structure,[10] are given in the Table I. The $E(\vec{k})$ dispersion curves are plotted in Fig. 2. The energies at high-symmetry points are analytical and we have reported them in the Appendix. Using a linear interpolation for the energies, we can calculate the density of states $n(E)$ by an extension of the tetrahedron method developed for the three-dimensional problem.[16] The calculated density of states is plotted in Fig. 3 for the parameters given in the Table I. But the two-center integrals vary with the interatomic distance. Owing to the exponential tail of atomic functions, one may use an exponential variation of the two-center integrals:

$$\beta=\beta_0\exp(-qR)\,, \tag{4}$$

where R is the interatomic distance. Using the density of states we can calculate the electron contribution E_A to the cohesive energy:

$$E_A=\int^{E_F} En(E)dE-2E_s-2E_p\,. \tag{5}$$

It is the difference between the one-electron energy of the graphite crystal and of the free atom. This energy is attractive and increases when the interatomic distance R decreases. To stabilize the crystal, one generally adds a repulsive term E_R at short distances owing to the interaction between the ions and to the atomic functions overlap that we have neglected in the tight-binding approximation. We set

$$E_R=N_v C_0\exp(-pR)\,, \tag{6}$$

where N_v is the coordination number (in graphite equal to 3). The parameters C_0, p, and q can be fitted to the experimental values of the cohesive energy E_c and of the stretching force constant,[12]

TABLE I. Values of the two-center integrals fitted to the Painter and Ellis band structure (Ref. 10) (in eV).

E_s	E_p	β	β'	β_c	β_t
−11.655	−7.711	−12.939	−1.165	−1.462	1.866

and also to the equilibrium condition

$$\left[\frac{dE_c}{dR}\right]_{R=R_0}=0\ , \tag{7}$$

where R_0 is the equilibrium interatomic distance (1.42 Å). Then

$$E_c=E_A+E_R\ . \tag{8}$$

Using such a model one generally finds, for the covalent elements, qR_0 close to 2, and pR_0 to 4.[17] This shows that the two-center integrals for non-near-neighbor atoms are small, and that the interaction between layers is very small.

As the valence bands of covalent systems is close to a nearly free-electron band scheme, an R^{-2} variation of the two-center integrals has also been used.[18] For small variations of the interatomic distance, both approximations are not very different provided qR_0 is close to 2.

The advantage of an R^{-2} law is that it only uses the bulk equilibrium condition and the stretching force constant to fit the parameters pR_0 and C_0. The cohesive energy is more difficult to calculate as it involves orthogonalization terms, or shifts of the atomic levels E_s and E_p between the free atom and the bulk graphite that we neglect in our band calculation, which, in fact, only uses the net difference E_s-E_p and assumes that the atomic functions are orthogonal. Nevertheless, such a variation also gives small values of the two-center integrals for atomic orbitals centered on different graphite layers. We shall below use this approximation to minimize the interstitial energy.

III. THE INTERSTITIAL CARBON ELECTRONIC STRUCTURE

A. Influence of the interstitial on the density of states

At very low interstitial concentration we can assume that there is no interaction between the interstitial atoms. Then we can study the electronic structure of only one carbon atom intercalated between the graphitic layers. The Green's-function formalism is well suited to study such localized problems.[13] Let us call H_0 the Hamiltonian of the graphite crystal plus the free carbon atom one. The intercalation of the carbon atom between the graphitic layers adds to this Hamiltonian a potential V that connects the interstitial states to the graphite ones. If we define the Green's operator G_0 as

$$G_0=\frac{1}{E-H_0+i\eta}\ , \tag{9}$$

where η is a positive infinitesimal, the variation $\Delta n(E)$ of the graphite density of states owing to the perturbation V is simply

$$\Delta n(E)=-\frac{2}{\pi}\frac{d}{dE}[\arg\det(I-G_0V)]\ , \tag{10}$$

or if we use the variation $\Delta N(E)$ of the number of states below the energy E,

$$\Delta N(E)=\int^E \Delta n(E')dE' \tag{11}$$

$$=-\frac{2}{\pi}\arg[\det(I-G_0V)]\ . \tag{12}$$

In the tight-binding basis we use, the potential V has nonzero elements only between the interstitial s and p states and the atomic orbitals centered on its nearest neighbors. Figure 4 shows the different values of the two-center integrals that connect the interstitial to its neighbors. Let us recall that here we use the R^{-2} variation. The interstitial has been taken at its experimental[8] position 1.2 Å above an hexagonal ring and about 2.2 Å below one atom in the other neighboring layer. This position above the center of a carbon ring has also been shown to be the most stable.[7,19] As the two-center integrals decrease with the distance, and as the interstitial only has one nearest neighbor in this more distant layer, we have considered only the interactions between the interstitial and the closest-layer neigh-

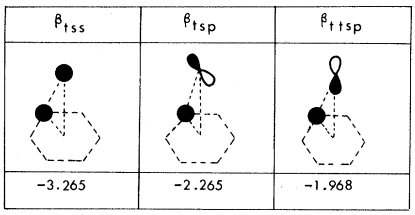

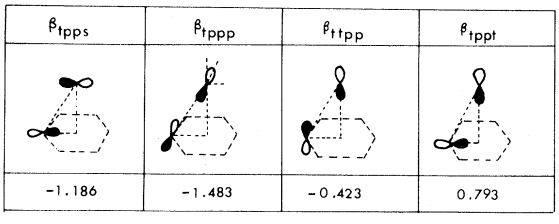

FIG. 4. Two-center integrals between the interstitial s and p states and its neighbors. An R^{-2} variation of the two-center integrals has been used to calculate their values from the graphite values.

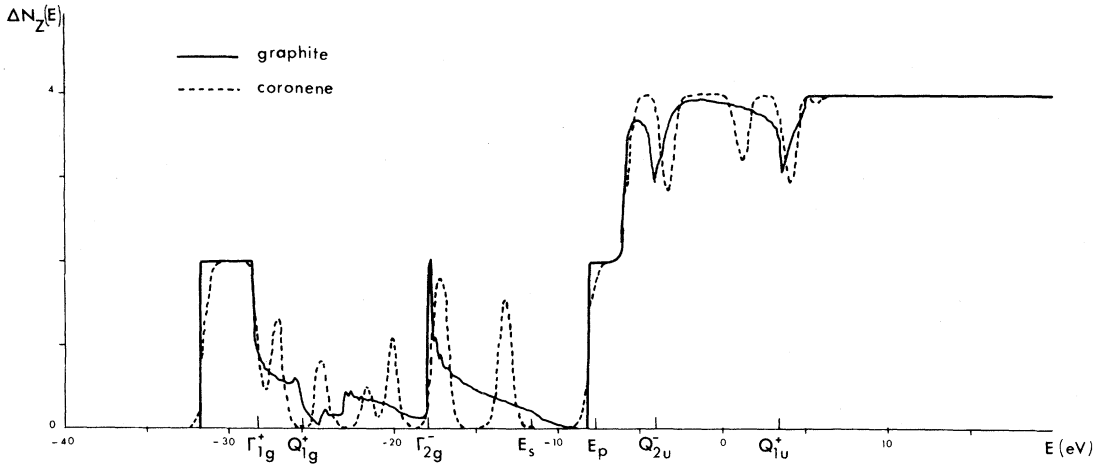

FIG. 5. Variation $\Delta N_z(E)$ of the graphite integrated density of states owing to the s and p_z interstitial orbitals.

bors. We shall also justify this approximation below considering the effect of these interactions.

Then V has nonzero elements between the s and p states on the interstitial and on its six neighbors. V is a 28×28 matrix that may be simplified using the symmetries of the problem. It is possible to separate the coupling of the graphite states with the interstitials s and p_z (normal to the graphite layers) orbitals and the one of the p_x (or p_y) states. The matrix V is then block-diagonalized into a 9×9 matrix V^z for the states of P_z symmetry, an 8×8 one V^x for the symmetry P_x, and a 6×6 one V^y for the symmetry P_y. There are also five states that do not couple with the interstitial states. Then one can easily show that

$$\Delta N(E)=\Delta N_z(E)+\Delta N_x(E)+\Delta N_y(E)\ , \tag{13}$$

where

$$\Delta N_i(E)=-\frac{2}{\pi}\arg\det(I-G_o^i V^i),\quad i=x,y,z\ . \tag{14}$$

Let us also note that, owing to the symmetry of the system, we have

$$\Delta N_x(E)=\Delta N_y(E)\ . \tag{15}$$

These variations of the integrated densities of states are plotted in Figs. 5 and 6.

In Fig. 5, we see that a localized state appears below the graphite bands. Let us note that this state is made of a symmetric combination of s graphite states on the interstitial neighbors, which were near the bottom of the band Γ_{1g}^+ in the absence of the interstitial. The same phenomenon arises at the bottom of the π band (level Γ_{2g}). A symmetric combination of π states is shifted below the band, owing to coupling with the s and p_z interstitial states. If one uses a second-order perturbation theory, it is then obvious that these interstitial states are repelled to higher energies. The effect is less important for the p_z state than for the s state of the interstitial atom, as the coupling of

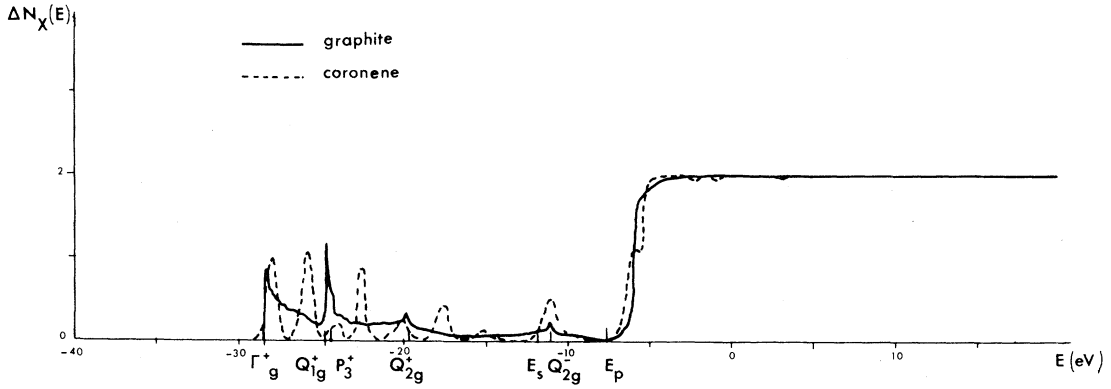

FIG. 6. Variation $\Delta N_x(E)$ of the graphite integrated density of states owing to the p_x (or p_y) interstitial orbitals.

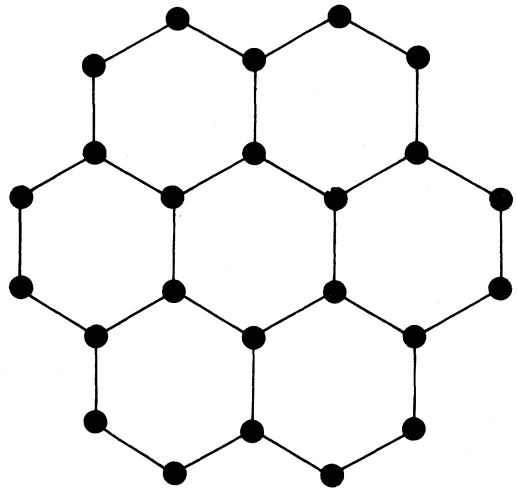

FIG. 7. Representation of a coronene molecule.

this last one is more important (Fig. 4).

Figure 6 shows that the coupling of the p_x or p_y interstitial states with the graphite ones is not very important. The p levels are slightly shifted upwards, owing to interactions with lower states in the graphite bands. These figures show that the coupling of the interstitial states is not very important. So this completely justifies the neglect of the two-center integrals between the interstitial and its single neighbor distant of 2.2 Å.

In the same figures we have also plotted the variation of the integrated density of states due to adsorption of a carbon atom at the middle of a coronene or hexabenzobenzene molecule (shown in Fig. 7). These results have been used as a test of our calculations. They are not very different from the graphite results, showing that there is no long-range effects and that the perturbations are strongly localized near the interstitial. Note that we have slightly broadened all the levels of the coronene molecule by Gaussians to get a continuous spectrum that we can compare with our preceding results.

In Fig. 8, we have plotted the total variation $\Delta N(E)$. One sees that the s and p states of the interstitial atom are now close to the graphite Fermi level. At this time, there is no observation of these states by photoemission spectroscopy or by energy-loss spectroscopy. But the variation of the density of states at about 4.3 eV (or 12 eV above the Fermi level) may be related to the variation of the secondary emission spectrum when a graphite crystal is bombarded by argon ions that create vacancies and interstitial atoms.[14]

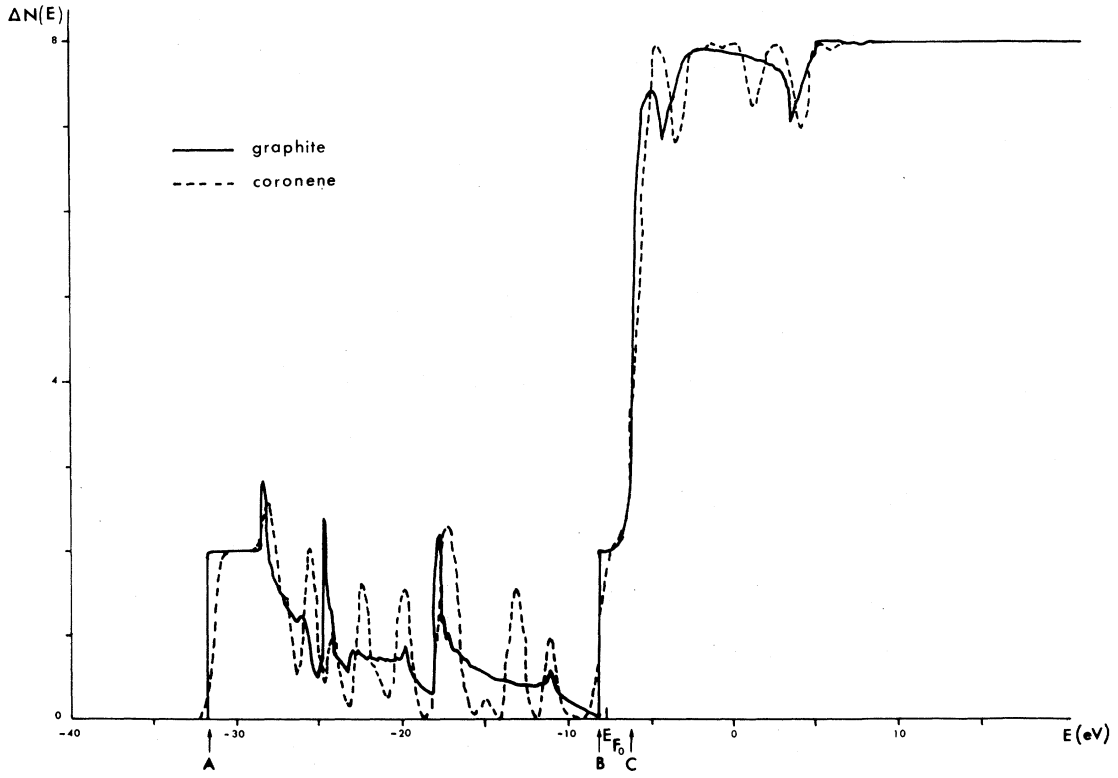

FIG. 8. Total variation $\Delta N(E)$ of the graphite integrated density of states owing to the interstitial.

B. Interstitial energy

We have already noted above that the graphite cohesive energy calculated by our model is larger than the experimental one. We get a value close to 23 eV instead of 7 eV. This is owing to the fact that we have assumed that the atomic orbitals are orthogonal. In fact this is not exactly true for free atom states. Orthogonalization terms would reduce our calculated value. As the interatomic distance between the interstitial and its neighbors is larger than the graphite equilibrium lattice constant, one can expect that the orthogonalization terms will be less important, as they decrease faster than the hopping integrals.

The electron contribution to the interstitial energy is the difference between the one-electron energies after and before the insertion of the carbon atom:

$$E_I = \int_{-\infty}^{E_F} E[Nn(E)+\delta n(E)]dE - \int_{-\infty}^{E_{F_0}} ENn(E)dE - 2E_s - 2E_p \ , \tag{16}$$

where E_F and E_{F_0} are the corresponding Fermi levels, N the number of graphite atoms, $n(E)$ the perfect graphite density of states (Fig. 3), and $\delta n(E)$ its variation due to the interstitial which has been calculated in III A. One can easily calculate the new position of the Fermi level:

$$\int_{-\infty}^{E_F}[Nn(E)+\delta n(E)]dE = \int_{-\infty}^{E_{F_0}} Nn(E)dE + 4 \ , \tag{17}$$

as the insertion brings four electrons. Thus we obtain

$$N\int_{E_{F_0}}^{E_F} n(E)dE + \int_{-\infty}^{E_F} \delta n(E)dE = 4 \ , \tag{18}$$

which shows that the difference $E_F - E_{F_0}$ is the order of $1/N$. Then the electron contribution to the interstitial energy is equal to

$$E_I = \int_{E_{F_0}}^{E_F} ENn(E)dE + \int_{-\infty}^{E_F} E\delta n(E)dE - 2E_s - 2E_p \ . \tag{19}$$

As $E_F - E_{F_0}$ is small, one can write

$$E_I \simeq \int_{E_{F_0}}^{E_F} E_{F_0} Nn(E)dE + \int_{-\infty}^{E_{F_0}} E\delta n(E)dE - 2E_s - 2E_p \ , \tag{20}$$

where the first term is calculated from (18). We derive

$$E_I = 4E_{F_0} + \int_{-\infty}^{E_{F_0}} (E - E_{F_0})\delta n(E)dE - 2E_s - 2E_p \ . \tag{21}$$

After an integration by parts the electron contribution to the interstitial energy is

$$E_I = 2(2E_{F_0} - 2E_s - 2E_p) - \int_{-\infty}^{E_{F_0}} \Delta N(E)dE \ , \tag{22}$$

where $\Delta N(E)$ has been calculated in the preceding section. Using, as in Sec. II, a R^{-2} variation of the hopping integrals, and the repulsive terms fitted to bulk properties but reduced, owing to a larger distance, we find an interstitial energy and an equilibrium position close to the experimental ones (Fig. 9).

This interstitial energy also depends on the graphite Fermi level E_{F_0}. Such a variation may be obtained in a substitutionally boron-doped graphite. Boron only has three s and p electrons. Its substitution to a carbon atom empties the graphite valence bands. Even with a small amount of boron the variation of the Fermi level is not negligible as the density of states at the perfect graphite Fermi level is equal to zero (in our model). One has measured a 0.2-eV variation for only 0.5 at. % B.[20] If we assume that the substitutional boron atoms do not modify the repulsion between the carbon atoms, we see in Fig. 10 that the electron contribution to the interstitial energy varies rapidly with the position of the Fermi level.

$\Delta N(E)$ is constant just below E_F and nearly

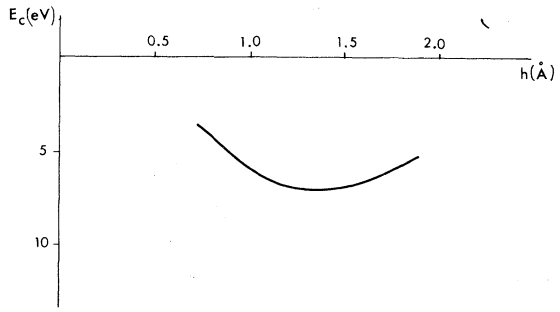

FIG. 9. Interstitial energy as a function of its distance to the graphite layer. The zero energy has been taken for no coupling between the interstitial and its neighbors. The experimental equilibrium position is equal to 1.2 Å.

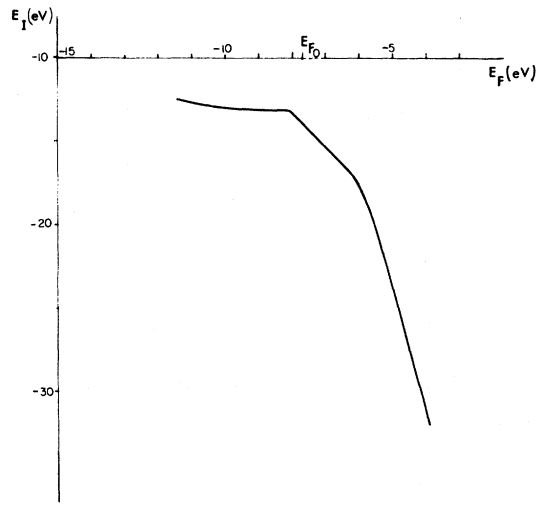

FIG. 10. Variation of the electron contribution to the interstitial energy as a function of the graphite Fermi level. (E_{F_0} is the Fermi level for pure graphite).

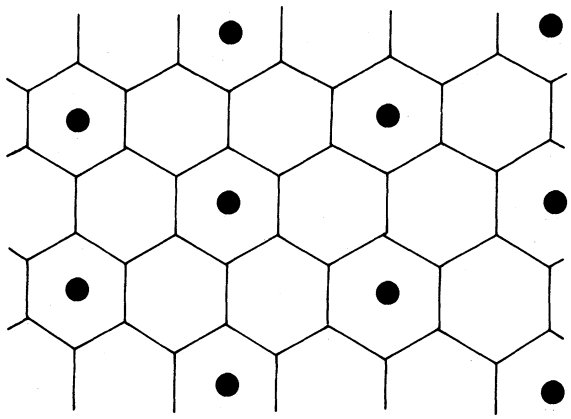

FIG. 11. This periodic arrangement gives a $\frac{1}{6}$ atomic concentration of interstitials.

equal to 2 (Fig. 7). So from Eq. (22) the interstitial energy is decreased by 0.4 eV for a Fermi-level variation of 0.2 eV. If the interstitial energy is close to the graphite cohesive energy as observed previously,[21] this can be sufficient to make the in-

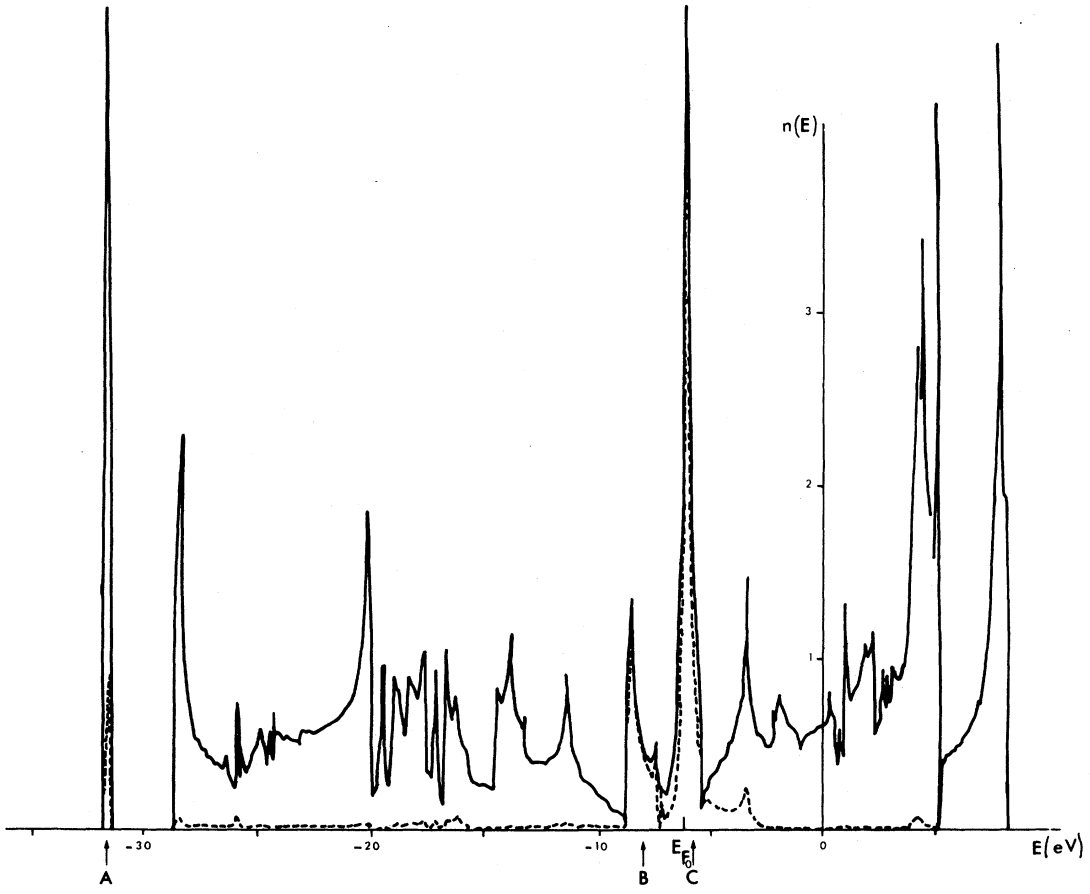

FIG. 12. Density of states for the interstitial atomic substructure given by Fig. 11. The dashed line gives the local density of states on the interstitials.

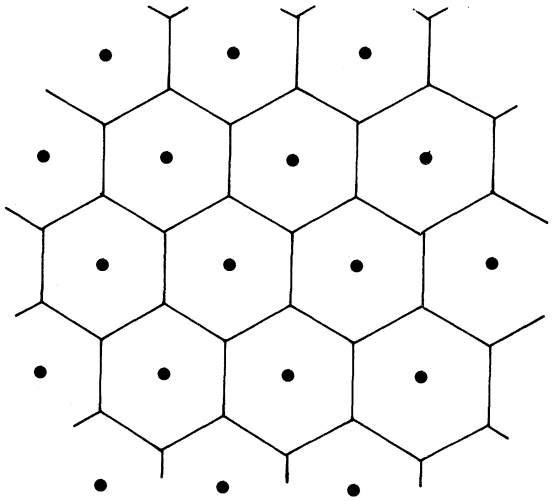

FIG. 13. Structure used for large interstitial concentration (50%).

terstitial unstable as it is observed experimentally[22] when one adds a small amount of boron to graphite. This gives good confidence in our interstitial electron structure and its large induced density of states near the graphite Fermi level. On the other hand, a donor substitutional impurity would stabilize the interstitial carbons.

IV. INTERSTITIAL INTERACTION

In the preceding section, we have studied the electronic structure of one isolated carbon interstitial in a graphite crystal. This is the case of a very small interstitial concentration. However, it seems that the measured interstitial concentration raises up to 10%.[15] Thus it is interesting to see if the interaction between the interstitials modifies the electronic structure obtained in the preceding section. This can be simply done if one studies a periodic arrangement of interstitials. There are several possibilities to simulate a concentration close to 10%. Nevertheless, even if the system is periodic, one cannot increase too much the number N of atoms in the unit cell, as we must diagonalize a $4N \times 4N$ Hermitian matrix for each wave vector in the Brillouin zone to get the energies $E(\vec{k})$. We have taken N equal to 7 and then an interstitial concentration equal to $\frac{1}{6}$ (Fig. 11).

The density of states is calculated by integration over the two-dimensional Brillouin zone, using an extension of the tetrahedron method previously developed for a three-dimensional one.[16] The density of states is plotted on Fig. 12. The localized state A that we obtained for an isolated interstitial is now slightly broadened in a band below the per-

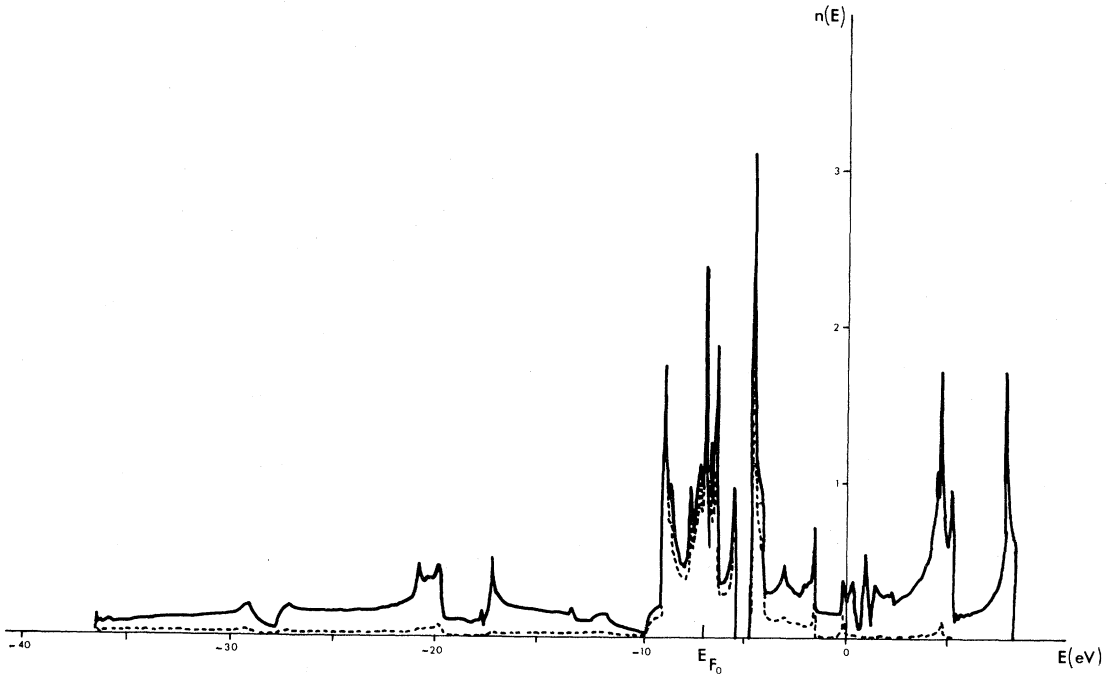

FIG. 14. Density of states for very large interstitial concentration. The dashed line gives the local density on states on the interstitials.

fect graphite bands. A large part of these states comes from the graphite. In contrast, the large densities of states near the Fermi level are made of interstitial s and p states. This is simply the same states as in Fig. 8 (B and C) which are also slightly broadened by the indirect interaction between the interstitials. So for a 16 at. % interstitial concentration, the interaction between the interstitials remains small. Then at the 10% experimental concentration, the mean distance between the interstitials will be of the same order of magnitude as in the configuration we have studied (Fig. 11). Nevertheless, some atoms may be closer. So we have studied a quite large interstitial concentration to see the effect of carbon interstitials above two neighbor carbon rings. This is the case of a 50% concentration (Fig. 13). The density of states is given on Fig. 14. The interaction between the interstitials is now sufficient to broaden the localized state appearing below the graphite bands for an isolated interstitial. The s and p interstitial states are also strongly broadened but the density of states at the Fermi level remains large. However, such a large local fluctuation of the concentration is not often expected as the measured concentration is only 10%.

V. CONCLUSION

In the tight-binding approximation, we have studied the electronic structure of carbon atoms intercalated between graphite layers. For a small concentration, the interstitials involve a large increase of the density of states near the graphite Fermi level. This can improve the electrical properties of graphite. Owing to this large density of states, the interstitial energy rapidly varies as one adds a small amount of boron substitutional impurities. On the other hand, a donor impurity would stabilize the interstitial: The calculated interstitial energy and position are in good agreement with the experimental values. We have also shown that the interaction between the interstitials is small.

APPENDIX

At high-symmetry points of the Brillouin zone, the tight-binding Hamiltonian may be diagonalized without the aid of a computer. In terms of the hopping integrals between sp_2 hydrized orbitals we get at the center of the Brillouin zone

$$E(\Gamma_{1g}^{+})=E_s+\beta+2\beta_t+2\beta_c+4\beta' ,$$

$$E(\Gamma_{3g}^{+})=E_p+\beta+2\beta_t-\beta_c-2\beta' ,$$

$$E(\Gamma_{3u}^{+})=E_p-\beta-2\beta_t+\beta_c+2\beta' ,$$

$$E(\Gamma_{1u}^{+})=E_s-\beta-2\beta_t-2\beta_c-4\beta' .$$

At the corner P and Q of the Brillouin zone, we have

$$E(P_3^{+})=\tfrac{1}{2}\{(E_s+E_p) \pm[(E_s-E_p)^2 +4(\beta-\beta_t-\beta_c+\beta')^2]^{1/2}\} ,$$

$$E(P_1^{+})=E_p\pm[(\beta-\beta_t)+2(\beta_c-\beta')] ,$$

$$E(Q_{1g}^{+})=\tfrac{1}{2}[(E_s+E_p)+2\beta_t -\beta_c+2\beta'\pm\sqrt{R_2}] ,$$

$$E(Q_{2g}^{+})=\tfrac{1}{2}[(E_s+E_p)-2\beta_t +\beta_c-2\beta'\pm\sqrt{R_1}] ,$$

$$E(Q_{1g}^{+})=E_p\pm(\beta+\beta_c-2\beta') ,$$

where

$$R_1=\left[\frac{E_p-E_s}{3}+2(\beta-\beta_t)-(\beta_c-2\beta')\right]^2 +8\left[\frac{E_s-E_p}{3}-\beta_c\right]^2 ,$$

$$R_2=\left[\frac{E_p-E_s}{3}-2(\beta-\beta_t)+(\beta_c-2\beta')\right]^2 +8\left[\frac{E_s-E_p}{3}+\beta_c\right]^2 .$$

*Equipe du LA 253 au CNRS.

[1]See, for instance, the various articles in *The Physics of Semimetals and Narrow Gap Semiconductors,* edited by D. L. Carter and R. T. Bate (Pergamon, New York, 1971).

[2]For a review see, for example, J. E. Fischer and T. E. Thompson, Phys. Today 31 (7), 36 (1978).

[3]L. A. Girifalco and N. A. W. Holzwarth, Mater. Sci. Eng. 31, 201 (1977).

[4]N. A. W. Holzwarth and S. Rabii, Mater. Sci. Eng. 31, 195 (1977).

[5]G. Volpilhac and J. Hoarau, J. Phys. C 13, 2281 (1980).

[6]I. L. Spain and D. J. Nagel, Mater Sci. Eng. 31, 183 (1977).
[7]A. Julg and M. Razman, Carbon 17, 335 (1979).
[8]J. P. Rouchy and L. Gatineau, Carbon 13, 267 (1975); 14, 97 (1976).
[9]F. J. Corbato, in *Proceedings of the Third Biennial Carbon Conference, Buffalo, 1957* (Pergamon, New York, 1959), p. 173.
[10]G. S. Painter and D. E. Ellis, Phys. Rev. B 1, 4747 (1970).
[11]R. F. Willis, B. Fitton, and G. S. Painter, Phys. Rev. B 9, 1926 (1974).
[12]A. Zunger, Phys. Rev. B 17, 626 (1978),
[13]J. C. Slater and G. F. Koster, Phys. Rev. 94, 1498 (1954).
[14]B. Lang, Surf. Sci. 66, 527 (1977).
[15]A. Pacault and A. Marchand, J. Chim. Phys. 1960, 873.
[16]J. Rath and A. J. Freeman, Phys. Rev. B 11, 2109 (1975).
[17]M. Lannoo, J. Phys. (Paris) 40, 461 (1979).
[18]S. Froyen and W. A. Harrison, Phys. Rev. B 20, 2420 (1979).
[19]A. J. Bennett, B. McCarroll, and R. P. Messmer, Phys. Rev. B 3, 1397 (1971).
[20]E. J. Mele and J. J. Ritsko, Phys. Rev. B 24, 1000 (1981).
[21]A. Pacault, in *Chemistry and Physics of Carbon,* edited by E. Walker (Dekker, New York, 1971), p. 107; D. Fishbach, *ibid.*, p. 1.
[22]J. P. Rouchy and J. Mering, C. R. Acad. Sci. 277, C533 (1973).